18th International Conference
ENGINEERING MECHANICS 2012
Svratka, Czech Republic, May 14 – 17, 2012
pp. 1229–1235
Paper #146

HYDRAULIC DESIGN OF INDUCER

J. Stejskal*

Abstract: *The paper deals with hydraulic design of an inducer. The mathematical model based on the Lagrange coordinates is presented. It is based on a choice of trajectory of a fluid particle in accordance with the continuity equation. Given the trajectory shape, it is possible to determine the specific energy of an inducer. The inducer blade is then determined by the family of these trajectories.*

Key words: ***Inducer, Euler equations, Continuity equation, Lagrange coordinates***

1 Introduction

When designing an inducer, the main criteria are high suction performance, high head rise and a positive pressure gradient. Currently, the design methods to avoid cavitation in inducers are becoming a major concern. This article provides relatively quick and easy methodology to do the preliminary blade design satisfying demanded parameters, while focus is put on suitable specific energy and pressure gradient. Cavitation in inducers is studied in papers (Rebattet et al 2001; Acosta et al 2001; Wegner et al 2003). No attempts to improve the cavitation performance have been made here.

2 Liquid Motion on a Helical Surface

Let us consider the helical surface in the coordinate system $\mathbf{x} = [x_1, x_2, x_3]$, as shown in Fig. 1.

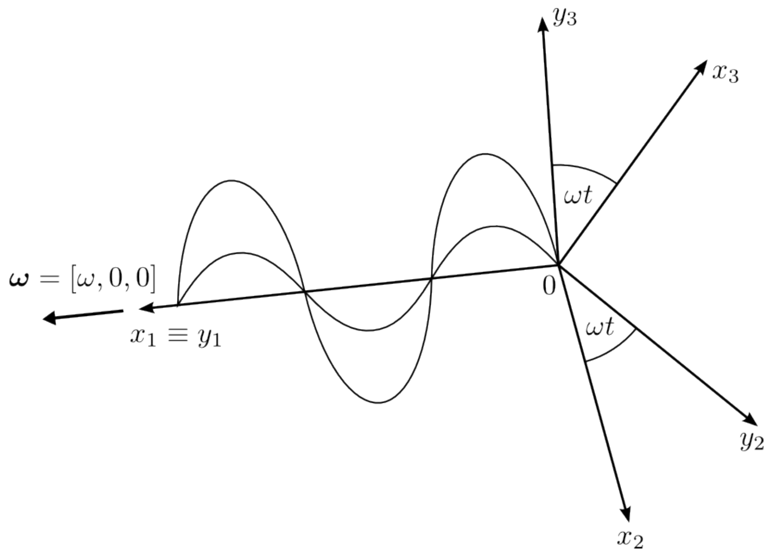

Fig. 1

This surface rotates around axis x_1 with angular velocity ω. We connect the rotating coordinate system $\mathbf{y} = [y_1, y_2, y_3]$ with the helix. In the system y_i we may write down the general parametric helical surface as

* Ing. Jiří Stejskal: Energy Institute, Brno University of Technology, Faculty of Mechanical Engineering, Technická 2896/2; 616 69, Brno; CZ, e-mail: jstejskal@gmail.com

$$y_2 = F(a_1, a_3) \cos A(a_1, a_2, a_3) \; ,$$
$$y_3 = F(a_1, a_3) \sin A(a_1, a_2, a_3) \; , \qquad (1)$$
$$y_1 = G(a_3) \, ,$$

where $a_1 \in \langle a_{1\mathrm{i}}, a_{1\mathrm{f}} \rangle$, $a_3 \in \langle 0, a_{3\mathrm{f}} \rangle$ and a_2 is fixed in the interval $\langle 0, 2\pi \rangle$. The relation between coordinates x_i and y_i is easily seen from Fig. 1. It holds that

$$x_2 = \cos(\omega t)\, y_2 - \sin(\omega t)\, y_3 \, ,$$
$$x_3 = \sin(\omega t)\, y_2 + \cos(\omega t)\, y_3 \, ,$$
$$x_1 = y_1 \, .$$

Substituting from (1), we have:

$$x_2 = F \cos(\omega t) \cos A - F \sin(\omega t) \sin A = F \cos(A + \omega t) \; ,$$
$$x_3 = F \sin(\omega t) \cos A - F \cos(\omega t) \sin A = F \sin(A + \omega t) \; , \qquad (2)$$
$$x_1 = y_1 \, .$$

Equations (1) define the shape of helix. To describe the motion of a fluid particle on this helix we choose the Lagrange coordinates, while this particle will be moving in the opposite direction of axis y_1, see Fig. 2. We will follow the motion of the fluid in time t from a certain point of the helix given by coordinates a_1, a_3. In general, this motion is described by

$$y_2 = F(a_1, a_3, t) \cos A(a_1, a_2, a_3, t) \, ,$$
$$y_3 = F(a_1, a_3, t) \sin A(a_1, a_2, a_3, t) \, ,$$
$$y_1 = G(a_3, t) \, .$$

To ensure that the particle follows the shape of the helix against the direction of axis y_1, we choose

$$y_2 = F(a_1, a_3 - \Omega t) \cos A(a_1, a_2, a_3 - \Omega t) \, ,$$
$$y_3 = F(a_1, a_3 - \Omega t) \sin A(a_1, a_2, a_3 - \Omega t) \, , \qquad (3)$$
$$y_1 = G(a_3 - \Omega t) \, ,$$

Where $t \in \langle 0, t_\mathrm{f} \rangle$ and Ω is the angular velocity of the fluid.

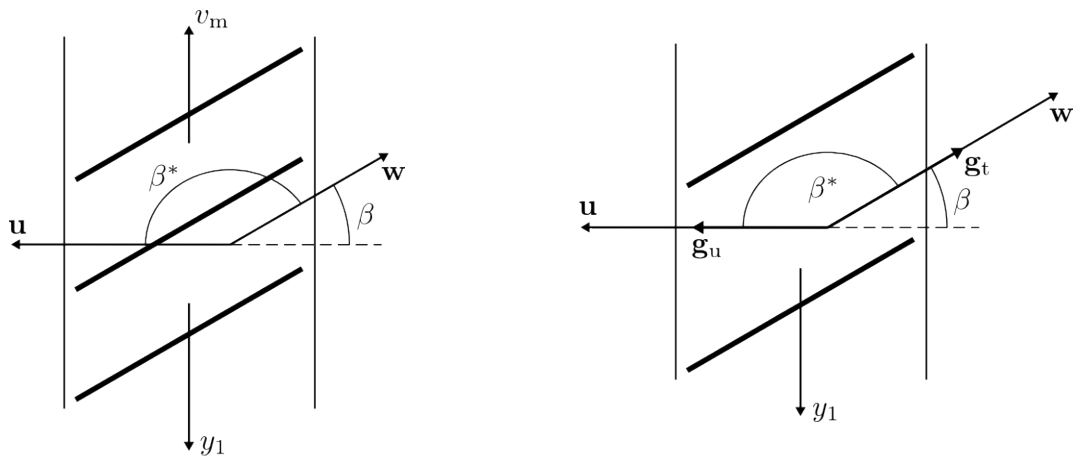

Fig. 2: Velocities and angles between them ($\mathbf{u}$ is the moving frame velocity, $\mathbf{w}$ is the relative velocity and v_m is the meridional velocity).

In system x_i, the fluid motion must satisfy the Continuity Equation (Brdička et al 2005), which in Lagrange coordinates takes the form $J(0) = J(t)$, where

$$J = \det \begin{bmatrix} \frac{\partial x_1}{\partial a_1} & \frac{\partial x_1}{\partial a_2} & \frac{\partial x_1}{\partial a_3} \\ \frac{\partial x_2}{\partial a_1} & \frac{\partial x_2}{\partial a_2} & \frac{\partial x_2}{\partial a_3} \\ \frac{\partial x_3}{\partial a_1} & \frac{\partial x_3}{\partial a_2} & \frac{\partial x_3}{\partial a_3} \end{bmatrix}.$$

Substituting from (2) and solving the determinant, we get

$$J(t) = F \frac{\partial F}{\partial a_1} \frac{\partial A}{\partial a_2} \frac{\partial G}{\partial a_3} = J(0)\,. \tag{4}$$

2.1 Important Relations for the Inducer Design

To determine the specific energy we need to know the circumferential velocity componentv_u. To set it down, let us do the time derivative of equations (2). Hence

$$\dot{x}_2 = \dot{F}\cos(A + \omega t) - F(\dot{A} + \omega)\sin(A + \omega t)\,,$$

$$\dot{x}_3 = \dot{F}\sin(A + \omega t) - F(\dot{A} + \omega)\cos(A + \omega t)\,,$$

where dot denotes the time derivative. Therefore, we have

$$v_\mathrm{u} = F(\dot{A} + \omega)\,, \tag{5}$$

$$v_\mathrm{r} = \dot{F}\,. \tag{6}$$

Now we determine the blade angle β. According to Fig. 2, we get

$$\cos\beta^* = \frac{\mathbf{g}_\mathrm{u} \cdot \mathbf{g}_\mathrm{t}}{\|\mathbf{g}_\mathrm{u}\|\|\mathbf{g}_\mathrm{t}\|}\,, \qquad \cos\beta = -\frac{\mathbf{g}_\mathrm{u} \cdot \mathbf{g}_\mathrm{t}}{\|\mathbf{g}_\mathrm{u}\|\|\mathbf{g}_\mathrm{t}\|}\,, \tag{7}$$

where $\mathbf{g}_\mathrm{u}$ is a vector in the direction of the moving frame velocity and $\mathbf{g}_\mathrm{t}$ is a vector tangential to the fluid particle trajectory. Obviously,

$$\mathbf{g}_\mathrm{u} = \begin{bmatrix} 0 \\ -F\sin A \\ F\cos A \end{bmatrix}, \qquad \mathbf{g}_\mathrm{t} = \begin{bmatrix} \dot{G} \\ \dot{F}\cos A - F\dot{A}\sin A \\ \dot{F}\sin A + F\dot{A}\cos A \end{bmatrix}.$$

Substituting these into (7), we obtain

$$\cos\beta = -\frac{F\dot{A}}{\sqrt{\dot{G}^2 + \dot{F}^2 + (F\dot{A})^2}}\,, \tag{8}$$

from where

$$\sin^2\beta = 1 - \cos^2\beta = \frac{\dot{G}^2 + \dot{F}^2}{\dot{G}^2 + \dot{F}^2 + (F\dot{A})^2}\,,$$

which implies

$$\mathrm{tg}\,\beta = -\frac{\sqrt{\dot{G}^2 + \dot{F}^2}}{F\dot{A}}\,. \tag{9}$$

2.2 Pressure

The pressure field can be determined from the Euler equations, which in Lagrange coordinates take the form (Brdička et al 2005)

$$\rho\frac{\partial^2 x_1}{\partial t^2}\frac{\partial x_1}{\partial a_k}+\rho\frac{\partial^2 x_2}{\partial t^2}\frac{\partial x_2}{\partial a_k}+\rho\frac{\partial^2 x_3}{\partial t^2}\frac{\partial x_3}{\partial a_k}=-\frac{\partial p}{\partial a_k}\,,\qquad k=1{,}2{,}3\,. \tag{10}$$

Using equations (2) in (10), we obtain equations describing the pressure field as

$$-\frac{\partial p}{\partial a_k}=\rho\left[\frac{\partial G}{\partial a_k}\ddot{G}+\frac{\partial F}{\partial a_k}\left(\ddot{F}-F\left(\dot{A}+\omega\right)^2\right)+\frac{\partial A}{\partial a_k}\left(2F\dot{F}\left(\dot{A}+\omega\right)+F^2\ddot{A}\right)\right]. \tag{11}$$

3 Results

The inducer blade for the following parameters was designed:

$$L=0{,}06\ \mathrm{m},\quad Q=6{,}94\,\frac{\mathrm{l}}{\mathrm{s}},\quad n=1450\ \mathrm{min}^{-1},\quad D_1=0{,}08\ \mathrm{m}\,,\quad D_2=0{,}04\ \mathrm{m}\,,$$

where D_1 and D_2 are inner and outer diameters, respectively. Other quantites are as follows:

$$S=\frac{\pi}{4}\left(D_1^2-D_2^2\right)=0{,}00377\ \mathrm{m}^2\,,\quad v_\mathrm{m}=\frac{Q}{S}=1{,}84\ \frac{\mathrm{m}}{\mathrm{s}}\,,\quad \omega=\frac{2\pi n}{60}=151{,}84\ \frac{\mathrm{rad}}{s}\,.$$

Resulting blade surface is in Fig. 3.

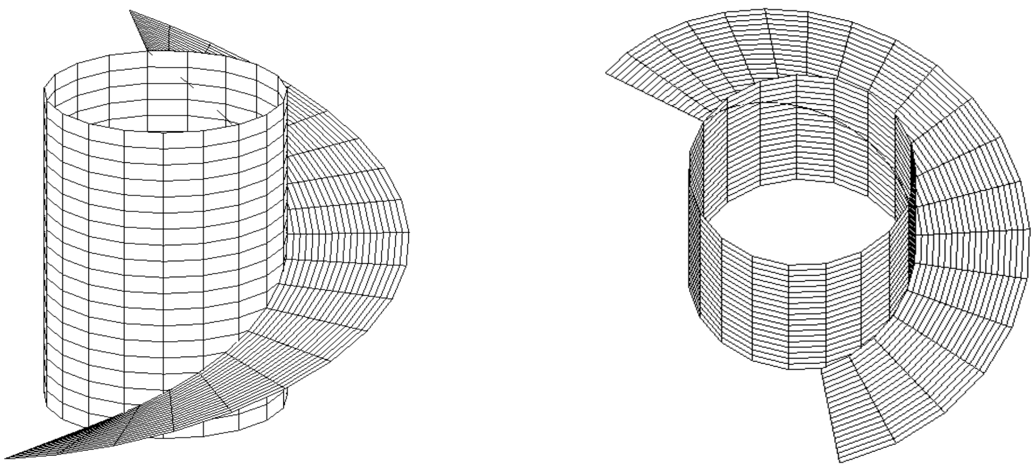

Fig. 3

Blade parameters in the mean region are:

$$v_{\mathrm{u}1}=0\,\frac{\mathrm{m}}{\mathrm{s}},\quad v_{\mathrm{u}2}=1{,}7\,\frac{\mathrm{m}}{\mathrm{s}},\quad Y=7{,}84\,\frac{\mathrm{J}}{\mathrm{kg}}\,,\quad H_{75\%}=0{,}5994\ \mathrm{m}\,,$$

where $H_{75\%}$ is the head at efficiency of 75%. To compare these results, numerical computations by the singularity method were performed. Results were obtained for 20 blades of zero thickness as an approximation to the infinite number of blades. It gives

$$r_{\mathrm{min}}:\quad \Delta p=2770\ \mathrm{Pa},\ \ H_{75\%}=0{,}2614\ \mathrm{m},$$

$$r_{\mathrm{mean}}:\quad \Delta p=6202\ \mathrm{Pa},\ \ H_{75\%}=0{,}5851\ \mathrm{m},$$

$$r_{\mathrm{max}}:\quad \Delta p=10996\ \mathrm{Pa},\ \ H_{75\%}=1{,}0368\ \mathrm{m},$$

This is a good approximation to the theoretical result.

As another example, the following inducer was designed (see Fig. 4):

$$L_{\max} = 0{,}14 \text{ m}, \;\; L_{\min} = 0{,}111 \text{ m}, \;\; Q = 616 \frac{\text{l}}{\text{s}}, \;\; n = 2980 \text{ min}^{-1},$$

$$D_1 = 0{,}306 \text{ m}, \;\; D_2 = 0{,}150 \text{ m} .$$

Resulting blade surface is in Fig. 5. Assuming the infinite number of blades, the head is

$$H_{75\%} = 38 \text{ m} .$$

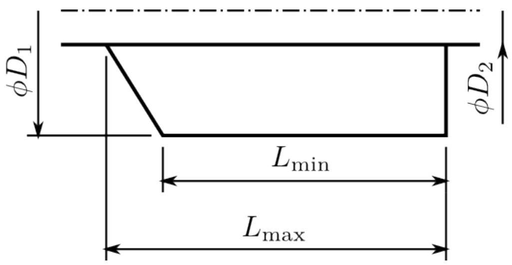

Fig. 4: Meridional section.

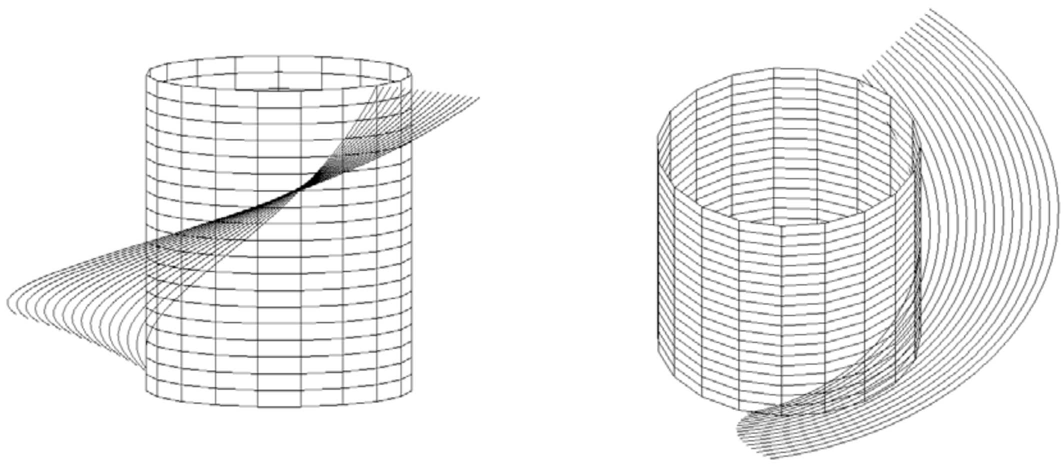

Fig. 5

This inducer was proceeded to a CFD computation. Its three dimensional model is in Fig. 6.

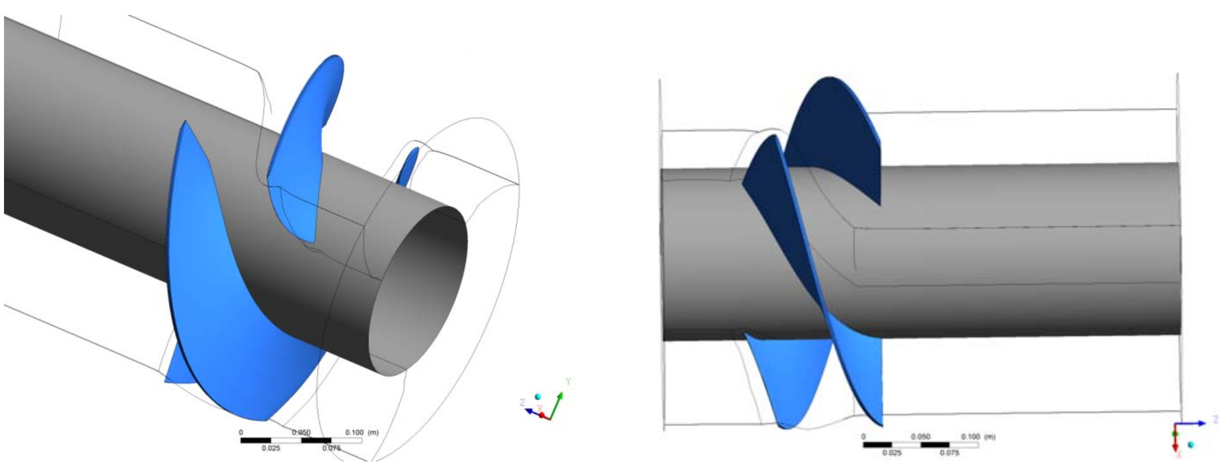

Fig. 6

From Fig. 7 we see that this inducer was designed with zero angle of incidence along the leading edge (Pochylý et al 2011). Head $H = 23{,}18$ m. The blade loading is in Fig. 8, from where the pressure difference between pressure and suction side of the blade can be seen. A value of the pressure in a point has no meaning, only differences are meaningful.

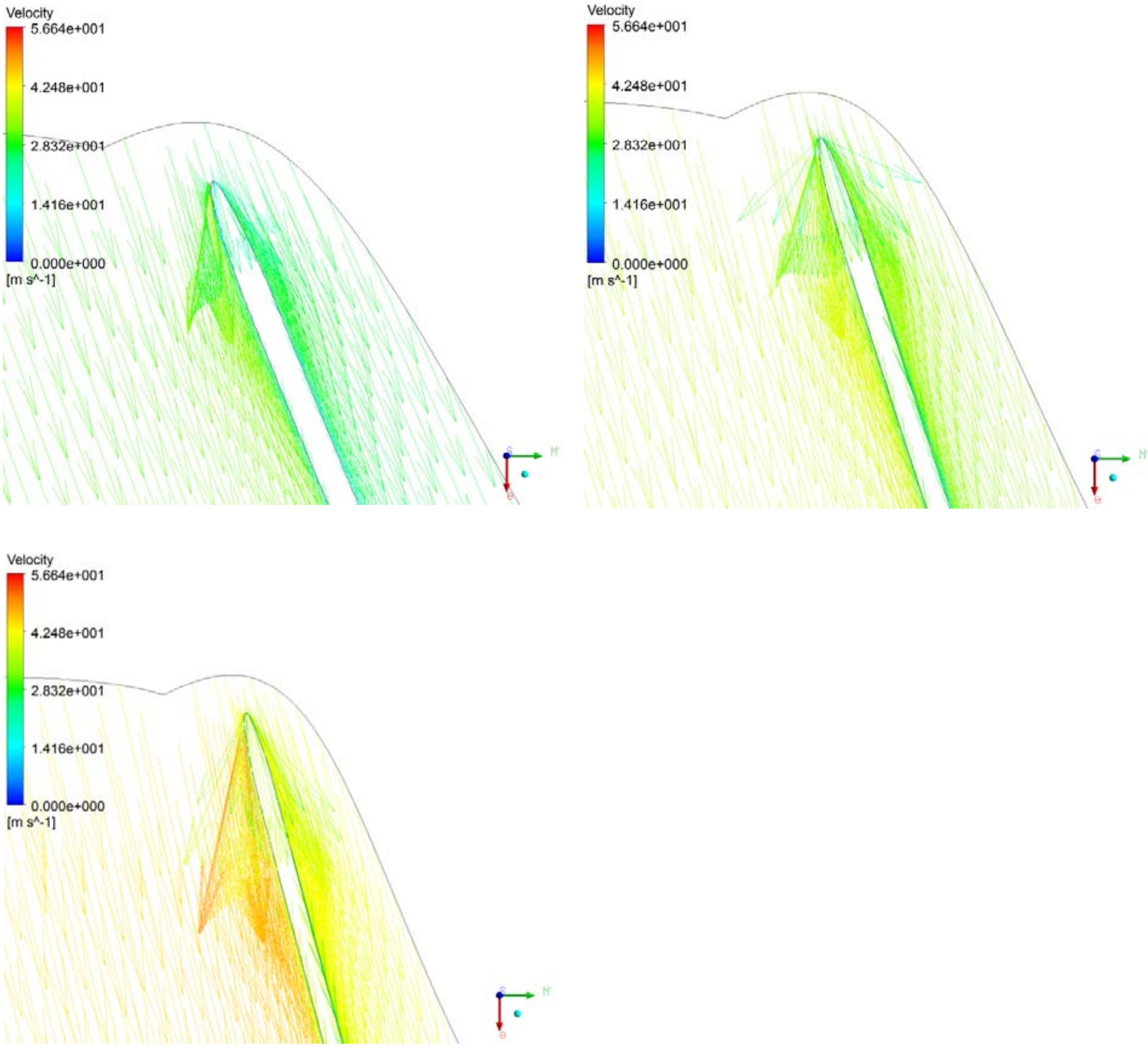

Fig. 7: Relative velocities at 20%, 50% *and* 80% *span between hub and tip.*

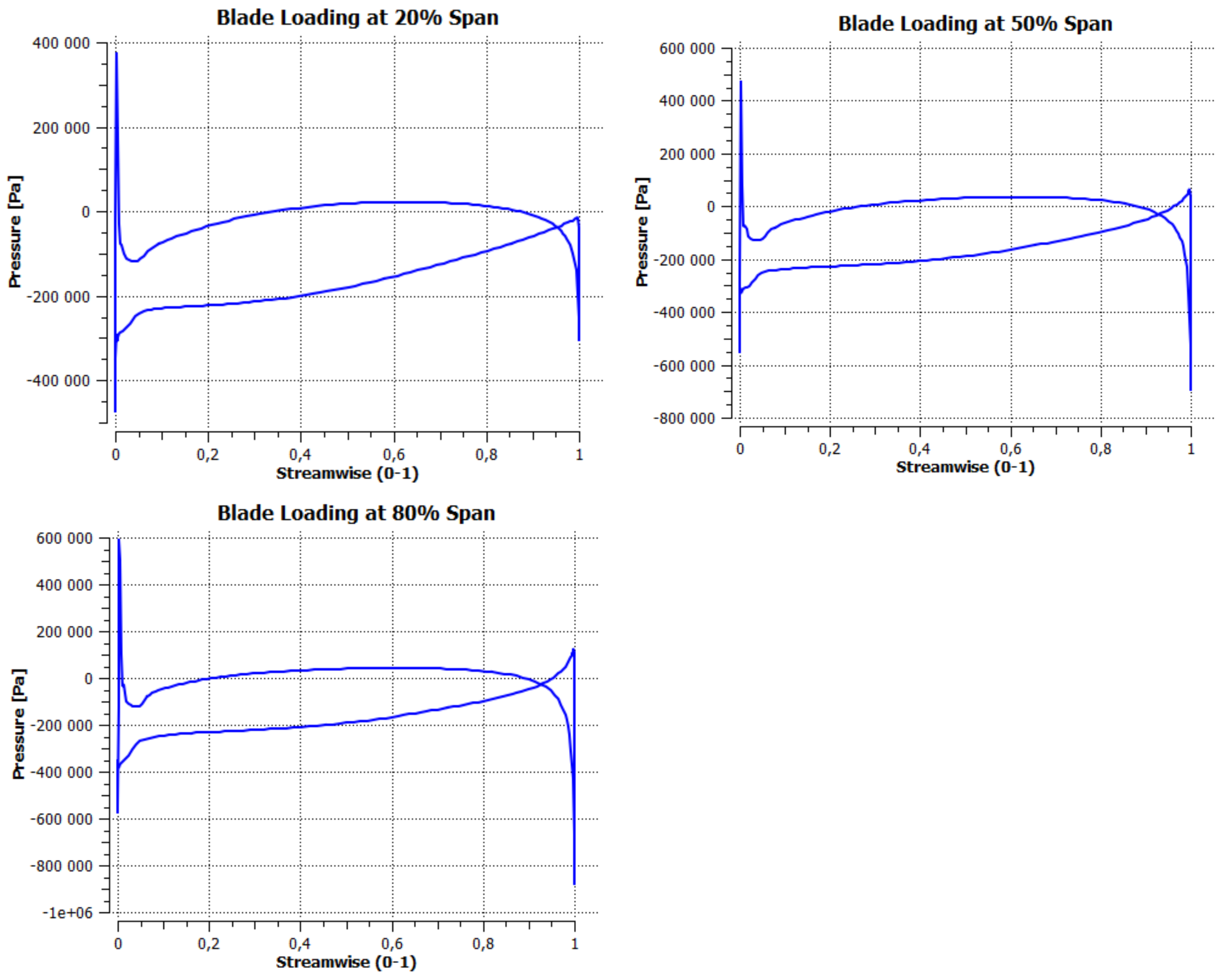

Fig. 8

4 Conclusions

This paper presents the methodology to design an inducer blade. It is based on Euler equations together with the continuity equation in Lagrange coordinates. It can be used to perform the preliminary blade design and to predict its parameters (specific energy, pressure gradient, etc.). Several inducers were designed and compared to numerical computations. It was shown that these numerical results are in good agreement with the presented theory.

Acknowledgement

The financial support of the Specified Research Grants No. FSI-J-12-21/1698, No. FSI-S-12-2 and NETME Centre project - New technologies for Mechanical Engineering CZ.1.05/2.1.00/01.0002 is gratefully acknowledged.

References

Rebattet, C., Wegner, M., Morel, P. & Bonhomme, Ch. (2001) *Inducer design that avoids rotating cavitation.* CREMHyG's research report.

Acosta, A. J., Tsujimoto, Y., Yoshida, Y., Azuma, S. & Cooper, P. (2001) Effects of Leading Edge Sweep on the Cavitating Characteristics of Inducer Pumps. *International Journal of Rotating Machinery*, 7(6), pp.397-404.

Wegner, M., Acosta, A. J. & Tsujimoto, Y. (2003) Panel Discussions on Inducer Design Criteria. *International Journal of Rotating Machinery*, 9, pp.229-237.

Pochylý, F., Stejskal, J., Haluza, M. & Rudolf, P. (2011) *Hydraulický návrh induceru.* Brno University of Technology research report No. VUT-EU 13303-QR-20-11.

Brdička, M., Samek, L. & Sopko, B. (2005) *Mechanika kontinua*. Academia, Praha.